Particle Filters and Beamforming for EEG Source Estimation

Petia Georgieva
Institute of Electrical Engineering and Telematics of Aveiro (IEETA)
Department of Electronics Telecommunications and Informatics (DETI)
University of Aveiro, Aveiro, Portugal
E-mails: petia@ua.pt

Lyudmila Mihaylova
School of Computing and Communications
Lancaster University, Lancaster, UK
E-mail: mila.mihaylova@lancaster.ac.uk

Nidhal Bouaynaya
Department of Systems Engineering
University of Arkansas at Little Rock, USA
E-mail: nxbouaynaya@ualr.edu

Lakhmi Jain
School of Electrical and Information Engineering, University of South Australia
Adelaide, Mawson Lakes Campus, South Australia SA 5095
E-mail: Lakhmi.jain@unisa.edu.au

Abstract—**This is a proof of concept work that proposes a solution to the inverse problem of EEG source estimation by combining two techniques, namely a Particle Filter (PF) for geometrical (3D) localization of the most active brain zones (expressed by two dipoles) and a beamformer (BF) as a spatial filter for estimation of the oscillations that have originated the recorded EEG data. The estimation is reliable for uncorrelated brain sources.**

Keywords-brain electrical source localization, filtering and state estimation, hidden markov models

I. INTRODUCTION

In brain imaging, the EEG source signal estimation is also known as the EEG inverse problem. The problem can be formulated as follows: using the measurements of electrical potential on the scalp recorded from multi-sensors, the goal is to build a reconstruction system able to estimate the location (the brain area) and the magnitude and directions of the dominative neural brain sources that most probably have originated the recorded EEG signal. Thus the problem can be divided in two stages: 1) localization of the principal original sources inside the brain; 2) estimation of the source signal (waveforms).

The problem of reconstructing the time pattern of the original source signals from a sensor array, can be expressed as a number of related Blind Source Separation (BSS) problems. In [1], a review of various BSS and independent component analysis (ICA) algorithms for static and dynamic models in their applications is presented. Beamforming (BF) is also a popular analysis procedure for non-invasive recorded electrophysiological data sets. The goal is to use a set or recording sensors and combine the signals recorded at individual sites to increase the signal-to-noise ratio, but focusing on a certain region in space (region-of-interest, ROI). In that sense, BF uses a different approach to image brain activities: the whole brain is scanned point by point. Thus, it is in fact a spatial filter designed to be fully sensitive to activity from the target location, while being as insensitive as possible to activity from other brain regions. This is achieved by constructing the spatial filter in an adaptive way, i.e., by taking into account the recorded data. More concretely, the BF is carried out by weighting the EEG signals, thereby adjusting their amplitudes such as that when added together they form the desired source signal.

In this paper we propose a solution to the brain electrical source localization combining two techniques, namely a Particle Filter (PF) for geometrical (3D) localization of the

most active brain zones and a beamformer (BF) as a spatial filter for estimation of the oscillations that have originated the recorder EEG measurements. The EEG inverse problem is intensively studded assuming that the source localization is known. In this work for the first time the problem of inverse modeling is solved simultaneously with the problem of the respective source space localization.

II. FILTERING AND STATE ESTIMATION – PROBABILISTIC FRAMERWORK

A. Hidden Markov Models (HMMs)

Hidden Markov Models (HMMs) are used to analyze or predict time series. HMMs and various probabilistic filters such as Kalman filters and Particle Filters (PF) are at the core of many deployed practical systems from elevators to airplanes. In general, every time there is a time series that involves noise, sensors or uncertainty, HMMs are the chosen algorithm to be applied. The essence of HMMs is the Markov chain. The Markov chain is a Bayes Network of a sequence of states $\{x_k, k \in \mathrm{N}\}$ that evolve over time, N is the set of natural numbers. Every state x_k is possibly a nonlinear function f of the previous state x_{k-1} and is also affected by the process noise sequence w_{k-1}

$$x_k = f(x_{k-1}, w_{k-1}), \tag{1}$$

The states are not directly observable, they are related with available measurements z_k (observable variables) through which the internal, hidden states can be inferred

$$z_k = h(x_k, v_k), \tag{2}$$

where h is possibly a nonlinear function and v_k is the measurement noise sequence. Expressions (1) and (2) are the state and the measurement equations of the general HMM [2]. It is assumed that the observations are taken as a time series, at discrete time points with a discretization time step T. Within this Bayesian framework, estimation and prediction problems can be formulated and solved. In prediction, the next state or the next measurement can be predicted, while state estimation means computing the probability of the internal (hidden) state given measurements. The estimation problem is to recursively calculate some degree of belief in the state x_k at time k, given the data $z_{1:k}$ up to time k [3]. Thus it is required to construct the posterior probability density function (pdf) $p(x_k \mid z_{1:k})$. It is assumed that the initial pdf $p(x_o \mid z_o) \equiv p(x_o)$ of the state vector, which is also known as the prior, is available (z_0 is the initial measurement). Then, the posterior conditional pdf $p(x_k \mid z_{1:k})$ may be obtained recursively, in two stages: prediction and update. Suppose that the required pdf $p(x_{k-1} \mid z_{1:k-1})$ at time k-1 is available. The prediction stage involves using the system model (1) to obtain the prior pdf of the state at time k via the Chapman-Kolmogorov equation

$$p(x_k \mid z_{1:k-1}) = \int p(x_k \mid x_{k-1}) p(x_{k-1} \mid z_{1:k-1}) dx_{k-1} \tag{3}$$

The probabilistic model of the state evolution $p(x_k \mid x_{k-1})$ is defined by the system equation (1) and the known statistics of w_{k-1}. At time step k, a measurement z_k becomes available and this may be used to update the prior (update stage) via the Bayes' rule.

$$p(x_k \mid z_{1:k}) = \frac{p(z_k \mid x_k) p(x_k \mid z_{1:k-1})}{p(z_k \mid z_{1:k-1})} \tag{4}$$

$p(z_k \mid z_{1:k-1})$ is a normalizing constant defined by the measurement model (2) and the known statistics of v_k. Hence, the recursive update of $p(x_k \mid z_k)$ is proportional ($\propto$ is the sign of proportionality)

$$p(x_k \mid z_{1:k}) \propto p(z_k \mid x_k) p(x_k \mid z_{1:k-1}). \tag{5}$$

In the update stage (4) the measurement is used to modify the prior density to obtain the required posterior density of the current state. Equations (3) and (4) form the math of a HMM.

B. Particle Filters (PFs)

In many real life problems the recursive propagation of the posterior density cannot be performed analytically (the integral in eq. (3) is intractable). Usually numerical methods are used and therefore a sample-based construction to represent the state pdf. The family of techniques that solve numerically the estimation problem are denoted as Particle Filters (PFs). The key idea of the PFs is the representation of the belief. The state space is discrete; it is a collection of points (also termed particles). Intuitively speaking, each particle is a representation of the possible state and after each iteration some of the particles survive other die in proportion to the measurement probability. The algorithm sets as an input a set of N particles with associated importance weights $W_k^{(l)}$ $l = 1,2,...,N$. Initially, the particles are spread out uniformly. The posterior probability $p(x_k \mid z_{1:k})$ is approximated by weighted sum of particles

$$\hat{p}(x_k \mid z_{1:k}) = \sum_{l=1}^{N} W_{k-1}^{(l)} \delta(x_k - x_k^l) \tag{6}$$

and the update probability is

$$p(x_k^{(l)} \mid z_{1:k}) = \sum_{l=1}^{N} \hat{W}_k^{(l)} \delta(x_k - x_k^{(l)}) \tag{7}$$

where

$$W_k^{(l)} = W_{k-1}^{(l)} p(z_k \mid x_k^{(l)}) \tag{8}$$

The normalized importance weights are

$$\hat{W}_k^{(l)} = W_k^{(l)} \Big/ \sum_{l=1}^{N} W_k^{(l)} \tag{9}$$

New states are calculated, putting more weight on particles that are important according to the *posterior* pdf (7). It is often impossible to sample directly from the posterior density function $p(x_k \mid z_{1:k})$. This difficulty is circumvented by making use of the importance sampling from a known *proposal distribution* $p(x_k \mid x_{k-1})$. During the prediction, stage each particle is modified according to the state model (1). In the update stage, each particle's weight is re-evaluated based on the new measurements.

C. Particle degeneracy

Typical numerical problem when applying the PF algorithm is the particle degeneracy, the case when a small set of particles (or even just one particle) have significant weights. An estimate of the measure of degeneracy, [4] at time *k* is given as

$$N_{eff} = \frac{1}{\sum_{l=1}^{N} \left(W_k^{(l)}\right)^2} \tag{10}$$

where N_{eff} is the number of (effective) particles with significant weights. If the value of N_{eff} is very low, a resampling procedure can help to avoid degeneracy. A schematic representation of the resampling procedure is depicted in Fig. 1 [5]. It shows on the left side 8 particles before resampling, where the diameters of the circles are proportional to the weights of the particles. The right hand side shows circles of the particles after the resampling step. The small particles are removed, while the large particles are replaced by particles with smaller weights. There are various mechanisms to perform the resampling step. Two of them are either resampling at each iteration or resampling when the effective number of particles falls below a user-defined threshold N_{eff}. The resampling step introduces variety in the particles, but increases the variance error of the particle population.

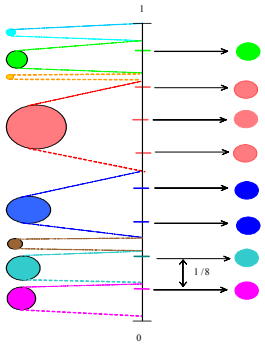

Figure 1. Particle resampling [5]

The above described HMM and PF concepts are applied in multiple fields like robotics, finance, language technologies, medicine, ect. For example there has been enormous progress in the field of speech decoding mostly due to HMMs that have been researched for more than twenty years and nowadays the state of the art in computer speech recognition uses variants of HMMs. PFs are one of the most successful algorithm in Artificial Intelligence (AI) and autonomous machine learning. In this paper we extend the application of the PF approach for brain electrical source localisation.

III. HMM OF THE BRAIN SOURCE LOCALIZATION PROBLEM

In order to apply the particle filter, outlined above, the HMM of the source localization has to be first defined.

A. Source Models: Dipoles and Multipoles

Let assume the brain activity arises at a small zone of the cortex centered at location x_s and that the observation point x is some distance away from this zone. The primary current distribution can be approximated by an equivalent current dipole represented as a point source $J^p(x_s) = s\delta(x - x_s)$, where $\delta(x)$ is the Dirac delta function, with moment $s \equiv \int J^p(x_s)dx_s$. The current dipole is an extension of the model of the paired-charges dipole in electrostatics. It is important to note that brain activity does not actually consist of discrete sets of physical current dipoles, but rather that the dipole is a convenient representation for coherent activation of a large number of pyramidal cells, possibly extending over a few square centimeters of gray matter. The current dipole model is the key of EEG processing since a primary current source of arbitrary extent can always be broken down into small regions, each region represented by an equivalent current dipole. However, an identification problem can arise when too many small regions and their dipoles are required to represent a single large region of coherent activation. These sources may be more simply represented by a multipolar model. The multipolar models can be generated by performing a Taylor series expansion of the function $G(x, x_s) = \dfrac{x - x_s}{\|x - x_s\|^3}$ about the centroid of the source. Successive terms in the expansion give rise to the multipolar components: dipole, quadrupole, octupole, and so on. In the present work the current dipole model is adopted.

B. Spherical Head Model

Computation of the scalp potentials requires a particular source model that has to be solved numerically. If the model is based on realistic head shapes, the computation can be a real challenge. Analytic solutions exist, however, for simplified geometries, such as when the head is assumed to consist of a set of nested concentric homogeneous spherical shells representing brain, skull, and scalp. These models are routinely used in most clinical and research applications to EEG source localization. Consider the special case of a current dipole with moment *s* located at x_s in a multishell spherical head, the scalp potential $z(x)$ measured at location x is

$$z(x) \approx a(\sigma_i)\frac{x \times x_q}{\left\|x - x_q\right\|^3} s \tag{11}$$

Assuming that the electrical activity of the brain can be modeled by a number of dipoles, i.e. the measured multichannel EEG signal signals $z_k \in \Re^{n_z}$ from n_z sensors at time k are produced by M dipoles, the forward EEG model is given by

$$z_k = \sum_{m=1}^{M} L_m(x_k(m))s_k(m) + v_k\,, \tag{12}$$

where $x_k(m)$ is a three dimensional localization vector (space directions), $L_m(x_k(m)) \in \Re^{n_z \times 3}$ is the lead field matrix for dipole m, $s_k(m)$ is a three dimensional moment vector of the mth dipole (the source signal). By v_k the effect of noise in the measurements is simulated. $L_m(x_k(m))$ is a nonlinear function of the dipole localization, electrodes positions and head geometry, [6]. Its three columns contain the activity that will be measured at the sensors due to a dipole source with unity moment in the x, y, and z directions, respectively, and zero moment in the other directions. An analytical expression for the forward model exists if the dipole localization, electrodes positions and head geometry are known. The spherical head model is the simplification that preserves some important electrical characteristics of the head, while reducing the mathematical complexity of the problem. The different electric conductivities of the several layers between the brain and the measuring surface need to be known. The skull is typically assumed to be more resistive than the brain and scalp that, in turn, have similar conductivity properties, [7]. In the framework of the dipole source localization problem, the states that have to be estimated are the geometrical positions of M dipoles $x_k = [x_k(1),.....x_k(M)]$, where

$$x_k(m) = [x(m), y(m), z(m)]^T\,,\ m = 1,...M \tag{13}$$

Then the lead field matrix of M dipoles $L_m(x_k) \in \Re^{n_z \times 3M}$ is

$$L(x_k) = [L(x_k(1)),.....L(x_k(M))] \tag{14}$$

The vector of moments $s_k \in \Re^{3M \times 1}$ is $s_k = [s_k(1),.....s_k(M)]^T$, where each $s_k(m)$ consists of brain source signals in each space direction, $s_k(m) = [s_x(m), s_y(m), s_z(m)]^T$. Eq. (12) can be reformulated in a matrix form as follows

$$z_k = L(x_k)s_k + v_k \tag{15}$$

Expression (15) corresponds to the measurement equation (2) of the HMM. As for the state equation (1), since it is unknown how the states (the geometrical positions of M dipoles) evolve over time, a random walk model (first-order Markov chain) is assumed in the source localization space,

$$x_k = x_{k-1} + w_k \tag{16}$$

Eqs. (15-16) define the dipole source localization model in state space. The intuition behind the PF approach is to estimate the 3D location (vector x) of the principle M dipoles (assuming M is known) that originated the underlying EEG recordings z_k . In the above model certain distributions for the process and the measurement noises are assumed and initial values for the states are chosen. The lead field matrix can then be computed, however the moments $s_k(m)$ are not known. In order to estimate them the beamforming approach is used.

C. Realistic Head Models

The EEG forward model, eq. (12), has a closed-form solution for heads with conductivity profiles that can be modeled as a set of nested concentric homogeneous and isotropic spheres. However, in reality, the human heads are anisotropic, inhomogeneous, and not spherical. Though the spherical models work reasonably well, more accurate solutions to the forward problem use anatomical information obtained from high-resolution volumetric brain images obtained with Magneto Resonance Images (MRI) or X-ray computed tomography (CT) imaging.

Many automated and semi-automated methods exist for surface extraction from MRIs The surfaces can then be included in a boundary element method (BEM) calculation of the forward fields. While this is an improvement on the spherical model, the BEM calculations are very time consuming and use of realistic head model may appear impractical when incorporated as part of an iterative inverse solution. In the present work, the spherical head model approach is chosen.

IV. Beamforming as a Spatial Filter

The Beamforming(BF) deals with the estimation of the time patterns in three space directions of mth current dipole

$$s_k(m) = [s_x(m), s_y(m), s_z(m)]^T$$

located at

$$x_k(m) = [x(m), y(m), z(m)]^T$$

using the measurements of electrical potential on the scalp recorded from N sensors located at the surface of the head. The BF filter consists of weight coefficients (B) that when multiplied by the electrode measurements give an estimate of the dipole moment at time k:

$$s_k = B^T z_k\,, \tag{17}$$

where $B \in \Re^{n_z \times 3M}$ is the weighting matrix. The choice of the beamformer weights is based on the statistics of the signal vector z_k received at the electrodes. Basically, the objective is to optimize the beamformer response with respect to a prescribed criterion, so that the output s contains minimal contribution from noise and interference. There are a number of criteria for choosing the optimum weights. The method described below represents a linear transformation where the transformation matrix is designed according to the solution of a constrained optimization problem (the early work is attributed to [8].

The basic approach consists in the following: assuming that the desired signal and its direction are both unknown, accurate signal estimation can be provided by minimizing the output signal variance. To ensure that the desired signal is passed with a specific (unity) gain, a constraint may be used so that the response of the beamformer to the desired signal is:

$$B^T L(x_k) = I\,, \tag{18}$$

where I denotes the identity matrix. Minimization of contributions to the output due to interference is accomplished by choosing the weights to minimize the variance of the filter output:

$$Var\{y_k\} = tr\{B^T R_{zk} B\} \tag{19}$$

where, $tr\{\ \}$ is the trace of the matrix in brackets, R_{zk} is the covariance matrix of the EEG signals. In practice, R_{zk} will be estimated from the EEG signals during a given time window. Therefore, the filter is derived by minimizing the output variance subject to the constraint defined in (19). This constraint ensures that the desired signal is passed with unit gain. Finally, the optimal solution can be derived by constrained minimization using Lagrange mltipliers [9] and it can be expressed as:

$$B^{opt} = R_{zk}^{-1} L^T(x_k)\left(L^T(x_k) R_{zk}^{-1} L(x_k)\right)^{-1} \tag{20}$$

The response of the beamformer is often called the linearly constrained minimum variance (LCMV) beamformer. The LCMV provides not only an estimate of the source activity, but also its orientation, reason why is classified as vector beamforming. The differences and similarities among beamformers based on this criterion for choosing the optimum weights are discussed in [10].

V. EXPERIMENTAL WORK

A. EEG simulation

EEG data was generated by eq. (12) at 30 scalp locations (Fp1, AF3, F7, F3, FC1, FC5, C3, CP1, CP5, P7, P3, Pz, PO3, O1, Oz, O2, PO4, P4, P8, CP6, CP2, C4, FC6, FC2, F4, F8, AF4, Fp2, Fz, Cz) covering the entire hemisphere according to the standard 10/20 International system (Fig. 2). In this study, we use a 3-sphere model to approximate the head geometry which includes three concentric layers for the brain, skull and scalp. The radii of the three concentric spheres are 8.7, 9.2 and 10 cm respectively and the corresponding conductivity values are 0.33, 0.0165 and 0.33 S/m. The origin of the reference coordinate system is located in the centre of the spheres with the x-axis pointing from right to left, the y-axis pointing back to front and the z-axis pointing bottom to top.

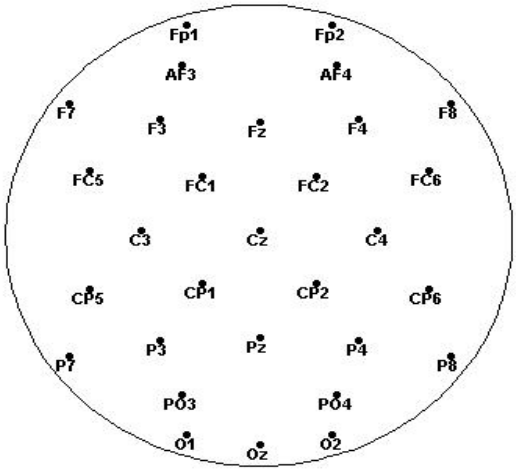

Figure 2. EEG electrode location according to the 10/20 Intern. system

The solution of the brain electrical source localization problem requires a significant number of forward model evaluations related with possible different source locations. Though these are relatively simple and fast computations, the multilayer spherical model is computed off-line by applying a grid based method to generate dipoles, assuming that the state space is discrete and consists of a finite number of states (dipoles). The dipoles are uniformly distributed in a sphere with radios 9 cm. Grids with varying dimensions are generated (25, 125, 512, 1140 uniformly distributed dipoles). Based on the grid of brain dipoles and the EEG electrode locations the Leadfield matrix $L(x)$ is computed off-line. The algorithm for EEG source estimation is summarized below. It is inspired by related works [11],[12].

B. EEG Source Estimation algorithm

for run =1, 2,..MC (Repeat the same algorithm MC number of runs)

Initialization

k=0, for $l = 1,2,...,N$

Generate N samples according to a chosen distribution $x_0^{(l)} \sim p(x_0)$ around initial vector $x_0 = \min(D) + \left(\max(D) - \min(D)\right) * rand(1, N)$.

Set initial weights $W_0^{(l)} = \frac{1}{N}$ (equal initial importance to all samples)

For k=1,2…

Prediction step

For $l = 1,2,...,N$ compute the state prediction according to the random walk state equation (19) $x_k = x_{k-1} + w_k$, where $w_k \sim \mathrm{N}(0,Q)$ is the process (assumed Gaussian) noise , $E[w_k w'_{k+j}] = 0$ for $j \neq 0$. The covariance matrix Q of w_k is $Q = \sigma_w^2 I$, I denotes the unit matrix and σ_w is the standard deviation. σ_w is chosen as a percentage (0-50%) from the previously estimated state vector x_{k-1} .

Beamforming step

i) Extract the underlying leadfield matrix from the complete $L(x_k)$ (computed off-line)

ii) Apply the BF technique to define the spatial filter w

iii) Compute the amplitudes at time k of the source signal propagated in 3 directions , for all estimated sources y_k

Measurement Update: evaluate the importance weights

for $l = 1,2,...,N$, on the receipt of a new measurement, compute the output according to the measurement equation (18) and compute the weights $W_k^{(l)} = W_{k-1}^{(l)} Lic\left(z_k \mid x_x^{(l)}\right)$

The likelihood is calculated as $Lic\left(z_k \mid x_x^{(l)}\right) \sim \mathrm{N}\left(h\left(x_k^{(l)}\right), \sigma_v\right)$

$$Lic\left(z_k \mid x_x^{(l)}\right) = \exp\left[-0.5 * (z_k - EEG_{data\_k}) R^{-1} (z_k - EEG_{data\_k})\right]$$

$$R = \mathrm{cov}(EEG_{data}) = \left(EEG_{data}\right)\left(EEG_{data}\right)^T =$$

for $l = 1,2,...,N$, normalize the weights $\hat{W}_k^{(l)} = W_k^{(l)} / \sum_{l=1}^{N} W_k^{(l)}$

Output

i) Calculate the posterior mean $E[x_k \mid z_{1:k}]$ as $\hat{x}_k = E[x_k \mid z_{1:k}] = \sum_{l=1}^{N} \hat{W}_k^{(l)} x_k^{(l)}$

ii) Compute the effective sample size $N_{eff} = \frac{1}{\sum_{l=1}^{N} \left(\hat{W}_k^{(l)}\right)^2}$

iii) if $N_{eff} < N_{tresh}$ do resampling

Multiply/suppress samples $x_k^{(l)}$ with high/low importance weights $\hat{W}_k^{(l)}$, in order to obtain N new random samples approximately distributed according to the posterior state distribution. The residual resembling algorithm, [4] is applied. Finally, weights are reset

for $l = 1,2,...,N$ set $W_k^{(l)} = \hat{W}_k^{(l)} = \frac{1}{N}$.

C. Source correlation test

The BF filter extracts reliably only noncorrelated neural sources. In order to generate EEG data originated by uncorrelated inner brain sources, the following correlation test is performed [13]. First, the covariance matrix in each direction is computed as

$$P_x = s(x)s(x)^T \in \Re^{qxq} , \quad (21)$$

where $s(x) \in \Re^{qxt}$ is a matrix with the source waveform in direction x of q active dipoles. The correlation factor is a matrix C_x , where each element is computed as

$$C_x^{(i,j)} = \frac{P_x(i,j)}{\sqrt{P_x(i,i)}\sqrt{P_x(j,j)}}, \quad i \neq j \ , \ C_x \in \Re^{qxq} \quad (22)$$

If $C_x^{(i,j)}$ is below a certain threshold, the correlation between signals $s_i(x)$ and $s_j(x)$ is significant. In the simulations, sin waveforms only in z direction with amplitude $a = 0.1$ and frequencies $f_1 = 10Hz$, $f_2 = 15Hz$ respectively are assumed for the two most active dipoles

$$Y_{true} = [0,\ 0,\ a\sin(2\pi f_1 t),\ 0,\ 0,\ a\sin(2\pi f_2 t)] . \quad (23)$$

The respective EEG signal, recorded with 1 kHz sampling rate (1000 samples per second), is generated by the following forward model

$$EEG_{noisy} = L(d_{true}) Y_{true} + v , \quad (24)$$

where

$v \sim \mathrm{N}(0, \sigma_v^2 I)$, $\sigma_v = \sqrt{\frac{Var\{L(d_{true}) Y_{true}\}}{SNR}}$, $L(d_{true}) \in \Re^{30 \times 3x2}$.

v reflects the effect of possible other brain active sources or non-cerebral activity like eye blinking, muscle contraction and other artifacts. The signal-to-noise ratio (SNR) is kept low, in the range of (-5, +5) dB, which corresponds to the real EEG SNR.

Since, the EEG is generated assuming two principal brain sources, the dimension of the state vector is $\mathbf{x} \in \Re^{6 \times 1}$ (three coordinates per dipole). The initial state vector $x_0 = [x_{10}, y_{10}, z_{10}, x_{20}, y_{20}, z_{20}]^T$ is randomly chosen from the defined dipole grid.

D. Tests

In all tests the number of the generated particles is N=500. Larger N leads to higher computational time however, decreasing N worsen the convergence. On Figures 3, 4 and 5 are summarized the results of the estimation errors $(d_{true} - d_{estimated})$ over the following scenarios:

Test 1: Grid of 25 dipoles, two active noncorrelated dipoles originated the simulated EEG data. Number of particles in the PF algorithm N=500. The algorithm has been repeated 10 times, the so called Monte Carlo (MC) runs.

Test 2: the same as Case 1 however EEG data was generated by correlated sources (threshold =0.05).

Test 3: Grid of 1140 dipoles, two active noncorrelated dipoles originated the simulated EEG data, N=500, 3 Monte Carlo runs.

Tests 1 and 2 are more proof of concept tests to verify that while the reconstruction of the noncorrelated sources (Fig 3) is practically without errors, the PF algorithm is not able to estimate correctly correlated sources (Fig.4). However, these cases are not realistic because the brain activity is limited to only 25 inner sources. For such low dimensional grid the distance between the dipoles is high (a coarse space grid) and in the lack of perturbations the estimation naturally converges. Though the higher dimensional grid space of Test 3 is associated with small steady state estimation errors (Fig. 5) it still converges to the true source coordinates for uncorrelated dipoles. A way to reduce the estimation error is to increase the number of the Monte Carlo runs (for example MC=100) and take the average of the errors. On Figures 6, 7 and 8 are depicted the recovered waveforms of the sources that originated the EEG data. In contrast to the correlated dipoles, the signal propagation at the uncorrelated dipoles are reliably estimated.

VI. CONCLUSIONS

This is a proof of concept work that pretends to solve the inverse problem of EEG source estimation by applying the mixture of Particle Filter (PF) and Beamforming (BF) approaches. The localization of two principle zones (expressed by two dipoles) are estimated starting from a number of randomly chosen initial guesses (particles). The estimation usually converges well for uncorrelated brain sources. Current research is focused on increasing the number of the estimated dipoles (more than two) and implementing the proposed technique for real EEG data. We are also working on comparison with the only tractable alternative of this work, a fully Bayesian approach (Variational Bayesian inversion) discussed in [14, 15, 16].

ACKNOWLEDGMENT

This work was supported by the Portuguese Foundation for Science and Technology under the grant SFRH/BSAB/1092/2010 and the Institute of Electronic Engineer-ing and Telematics of Aveiro (IEETA), Portugal.

REFERENCES

[1] S. Choi, A. Cichocki, H.M. Park, S.Y. Lee, "Blind Source Separation and Independent Component Analysis: A Review", Neural Information Processing, vol. 6(1), pp.1-57, 2005.

[2] P. Brasnett, L. Mihaylova, D. Bull and N Canagarajah, "Sequential Monte Carlo Tracking by Fusing Multiple Cues in Video Sequences, Image and Vision Computing", Elsevier Science, Vol. 25, No. 8, pp. 1217-1227, 2007.

[3] M. Arulampalam, S. Maskell, N. Gordon, T. Clapp, A tutorial on particle filters for online nonlinear/non-Gaussian Bayesian tracking, IEEE Transactions on Signal Processing, vol. 50, no. 2, pp. 174–188, 2002.

[4] J. Liu and R. Chen, "Sequential Monte Carlo methods for dynamic systems", Journal of the American Statistical Association vol. 93 (443) , pp.1032–1044, 1998.

[5] P. M. Djuric, J. H. Kotecha, J. Zhang, Y. Huang, T. Ghirmai, M. Bugallo, and J. Mıguez, "Applications of particle filtering to selected problems in communications," IEEE Signal Processing Magazine, vol. 20, no. 5, pp. 19–38, Sept. 2003.

[6] Y. Salu, L.G. Cohen, D. Rose, S. Sxato, C. Kufta, and M. Hallett, "An improved method for localizing electric brain dipoles," IEEE Transactions on Biomedical Engineering, vol. 37, no. 7, pp. 699 –705, july 1990.

[7] Y. Lai, W. van Drongelen, L. Ding, K. E. Hecox, V. L. Towle, D. M. Frim, and B. He, "Estimation of in vivo human brain-to-skull conductivity ratio from simultaneous extra- and intracranial electrical potential recordings," Clinical Neurophysiology, vol. 116, no. 2, pp. 456–65, 2005.

[8] Capon, J.: High-resolution Frequency Wavenumber Spectrum Analysis", Proceedings of the IEEE, 57: 1408-1418, (1969)

[9] Van Veen, B.D., van Drongelen, W., Yuchtman, M., Suzuki, A.: Localization of Brain Electrical Activity via Linearly Constrained Minimum Variance Spatial Filtering", IEEE Transactions on Biomedical Engineering, 44(9), (1997), 867-880.

[10] Huang, M-X., Shih, J.J., Lee, R.R., Harrington, D.L., Thoma, R.J., Weisend, M.P., Hanion, F., Paulson, K.M., Li, T., Martin, K., Miller, G.a., Canive, J.M.: Commonalities and Differences Among Vectorized Beamformers in Electromagnetic Source Imaging", Brain Topography, 16, (2004), 139-158.

[11] Mohseni H. R., Ghaderi F., Wilding E.L., Saeid Sanei, S.: A beamforming particle filter for EEG dipole source localization, International Conference on Acoustics, Speech, and Signal Processing (ICASSP) (2009) 337--340

[12] Mohseni H. R., Nazarpour, K., Wilding E.L., Saeid Sanei, S.: The application of particle filters in single trial event-related potential estimation, Physiol. Meas. 30 (2009a) 1101–1116

[13] A. M. Tomé, A.R. Teixeira, N. Figueiredo, I.M. Santos, P. Georgieva, E. Lang, "SSA of biomedical signals: A linear invariant systems approach", Statistics and Its Interface, Vol. 3, pp. 345–355, 2010.

[14] S. J. Kiebel, J. Daunizeau, C. Phillips, and K. J. Friston, Variational bayesian inversion of the equivalent current dipole model in EEG/MEG," NeuroImage, vol. 39, no. 2, pp. 728-741, Jan. 2008

[15] H. D. Ouden, J. Daunizeau, J. Roiser, K. J. Friston, and K. E. Stephan, Striatal prediction error modulates cortical coupling, Journal of Neuroscience, vol. 30, no. 9, pp. 3210-3219, 2010.

[16] V. Litvak and K. Friston, Electromagnetic source reconstruction for group studies," NeuroImage, vol. 42, no. 4, pp. 1490-1498, October 2008.

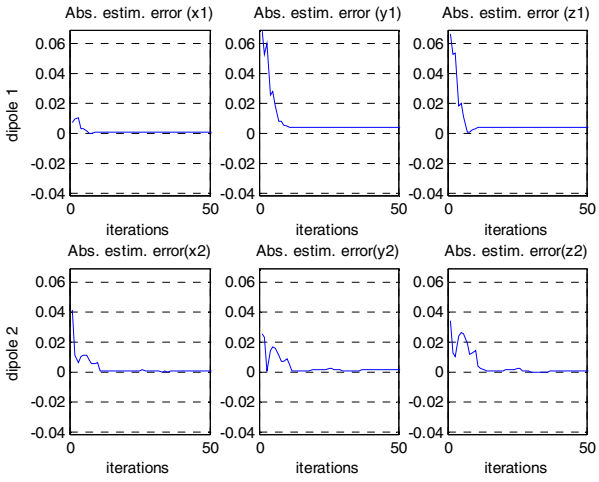

Figure 3. The absolute estimation error of the dipole location (Test 1)

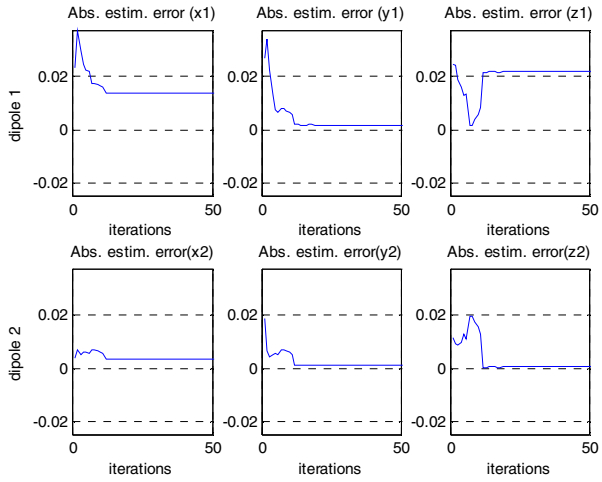

Figure 4. The absolute estimation error of the dipole location (Test 2)

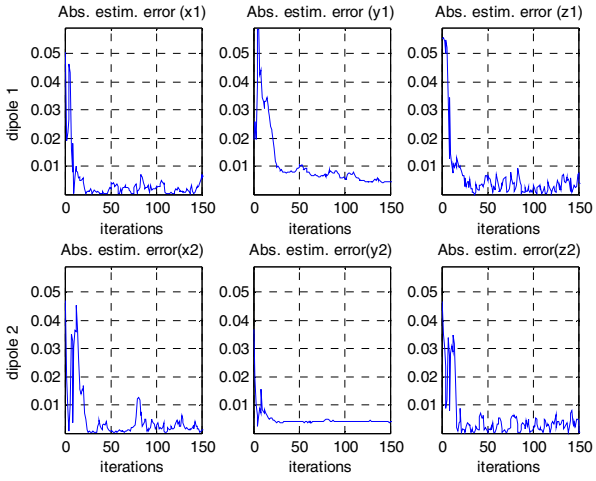

Figure 5. The absolute estimation error of the dipole location (Test 3)

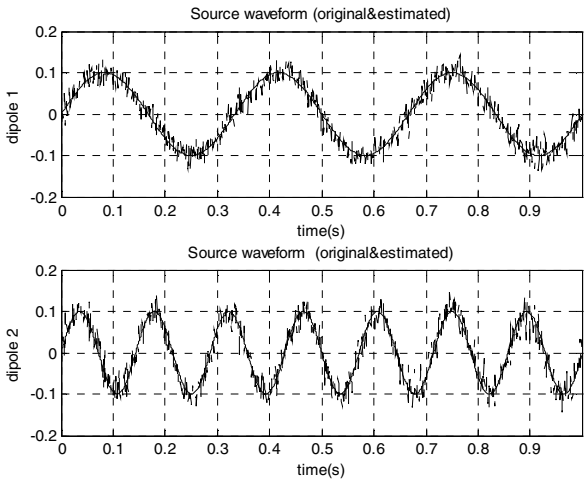

Figure 6. BF source waveform estimation (Test 1)

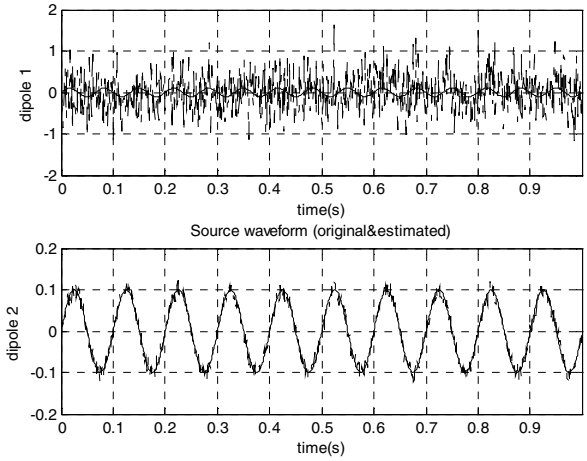

Figure 7. BF source waveform estimation (Test 2)

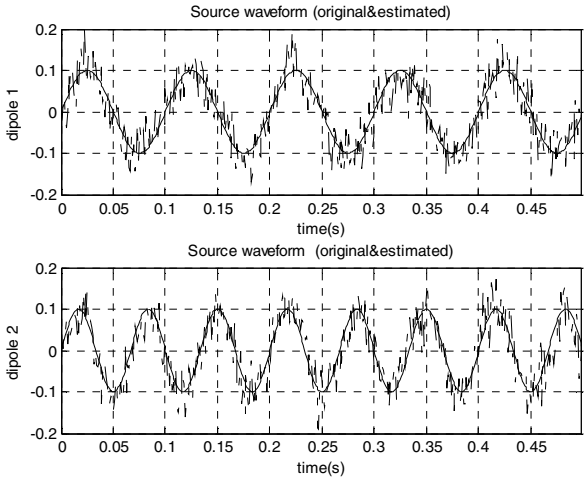

Figure 8. BF source waveform estimation (Test 3)